

Controlled many-body interactions in a frozen Rydberg gas

I. Mourachko, Wenhui Li, and T. F. Gallagher

Department of Physics, University of Virginia, Charlottesville, Virginia 22904, USA

(Received 25 November 2003; published 13 September 2004; publisher error corrected 29 September 2004)

Previous resonant dipole-dipole energy-transfer experiments of cold Rydberg gases [Anderson *et al.*, Phys. Rev. Lett. **80**, 249 (1998); Mourachko *et al.*, Phys. Rev. Lett. **80**, 253 (1998)] have been interpreted as providing evidence of many-body, as opposed to purely binary, effects. Here we separate two-body and many-body interactions by introducing an additional Rydberg state, which does not participate directly in the energy-transfer process, but is strongly coupled to one of the final states. We observe broadening of the energy-transfer resonances due to this added Rydberg state, which clearly demonstrates the many-body nature of the dipole-dipole interactions in such a system.

DOI: 10.1103/PhysRevA.70.031401

PACS number(s): 32.80.Pj, 34.60.+z

The cold dense sample of Rydberg atoms, which can be formed starting from atoms in a magneto-optical trap (MOT), is a gas. However, because it is so cold and there are strong interactions between Rydberg atoms, it exhibits fascinating collective properties normally associated with other systems [1,2]. For example, it can spontaneously evolve into an ultracold plasma [3,4], a transition roughly analogous to an insulator-metal transition. A second example, the topic of this paper, is resonant dipole-dipole energy transfer. In a gas it normally occurs by binary collisions, even at temperatures as low as 1 K [5]. Using the 300- μ K Rb Rydberg atoms in a MOT, we observe resonant energy transfer which appears superficially similar to that seen in a room temperature gas, but there is a fundamental difference. At a temperature of 300 μ K, the Rb Rydberg atoms move only a few percent of the typical interatomic spacing in the 1- μ s duration of the experiment. Consequently, in such a “frozen” Rydberg gas the observed energy transfer cannot occur by binary collisions, but rather by the interactions between static atoms. However, the widths of the observed resonances are more than an order of magnitude wider than is possible if due only to the binary dipole-dipole interactions between nearest neighbors at the average spacing. The observed widths have been attributed to the simultaneous interactions between many static atoms, as in an amorphous solid. Here we report a direct experimental demonstration of the importance of many-body interactions in the observed resonant energy transfer. A clear understanding of such interactions is essential for further exploration of a variety of interesting phenomena in cold dense Rydberg samples, such as superradiance [6], and quantum computation [7,8]. In the following sections we first outline the previous energy-transfer experiment, describe this experiment, and provide a theoretical sketch of the underlying physics.

The observed resonant energy transfer can be understood with the aid of Fig. 1. Cold, 300 μ K, Rb atoms are excited to the 33s and 25s states, and the energy transfer



can be tuned into resonance by an electric field [1]. There are two resonances, at the electric fields $E=3.0$ and 3.4 V/cm, due to the Stark splitting of the $|m_j|=\frac{1}{2}, \frac{3}{2}$ levels of the $34p_{3/2}$

state, as shown in the energy-level diagram Fig. 1(a). Unlike collisional resonances observed in higher temperature Rydberg samples, the linewidths of the resonances are density dependent, an observation consistent with static interactions between atoms. From the dipole moments $\mu=e\langle 25s|z|24p\rangle \approx 492$ a.u. and $\mu'=e\langle 33s|z|34p\rangle \approx 126$ a.u., it is straightforward to calculate the dipole-dipole interaction $V_1=\mu\mu'/R_0^3$ between atoms at the average spacing R_0 . The value $\mu\mu'/R_0^3=0.3$ MHz is far smaller than the observed 8-MHz width in [1], which has been attributed to the presence of the always resonant interactions



and

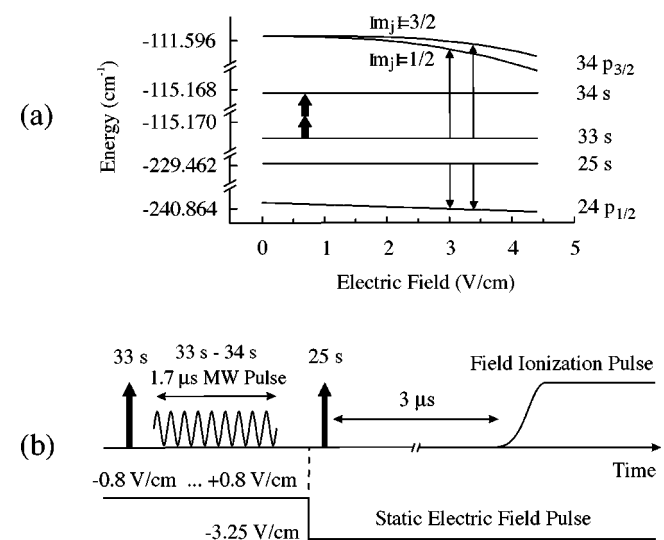
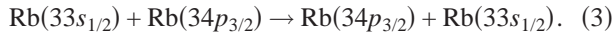
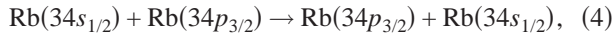


FIG. 1. (a) Energy-level diagram of an isolated Rb atom in an electric field. The arrows show the two energy-transfer resonances. The thick arrows indicate the two-photon microwave transition. (b) Timing of the lasers, microwave, and electric-field pulses for the experiment. The total electric-field is the sum of the electric field pulse applied 100 ns after the microwave pulse and low sweeping dc electric field.



The interactions of Eqs. (2) and (3) can be expected to broaden the observed resonances, because they split the final states of Eq. (1) into many states covering a range of energy. Due to the fact that the $25s$ and $33s$ states are important to both the fundamental energy-transfer process of Eq. (1) and the many-body broadening interactions of Eqs. (2) and (3), starting with only these two states, it is difficult to demonstrate experimentally the importance of the interactions of Eqs. (2) and (3). In this experiment, we have added the $34s$ state, which plays no role in Eq. (1), but adds another always resonant dipole-dipole interaction,



analogous to the interactions of Eqs. (2) and (3). Due to the large matrix element $\mu'' = e \langle 34s | z | 34p \rangle \approx 930$ a.u., even a relatively small number of $34s$ atoms leads to a readily observable broadening of the energy-transfer resonance.

The experiment is easily understood by referring to the energy level and timing diagrams of Fig. 1. The experimental approach has been described in detail in [9], therefore only a short description will be given here. The cold ^{85}Rb atoms are held in a vapor-loaded MOT, in which the density of cold atoms is about 5×10^{10} atoms/cm³ and the temperature about 300 μK . A Nd:YAG pumped dye laser is used to excite cold ^{85}Rb atoms from the $5p_{3/2}$ state to the $33s$ state, with maximum 10% excitation efficiency. Then, a 1.7- μs -duration microwave pulse transfers atoms from the $33s$ to the $34s$ state through a two-photon transition [9]. The frequency of the microwave pulse is fixed at 117.537 GHz, while the power can be varied to control the $34s$ population. The width of this transition is about 600 kHz, the transform limit of the pulse, in spite of the 10 G/cm inhomogeneity of the trap's magnetic field [9]. Therefore the excitation of the $34s$ state is efficient and relatively uniform throughout the sample. At the maximum power of the microwaves we excite about 20% of the $33s$ atoms to the $34s$ state. Due to the inhomogeneity in the B field and the randomness of the atomic spacings, we assume that any coherence between the $33s$ and $34s$ state is unimportant. As shown by Fig. 1(b), the microwave transition takes place in a dc field which is slowly scanned from -0.8 to $+0.8$ V/cm, a field small enough to not shift the $33s$ - $34s$ transition out of resonance. The $25s$ -state atoms are then excited from the $5p_{3/2}$ state with a second dye laser, with up to 10% efficiency as well. An electric-field pulse with 3.25 V/cm amplitude is applied just before the $25s$ excitation, and the system evolves in the presence of the combined static and pulsed fields. Scanning the dc field from -0.8 to 0.8 V/cm scans the total field from 2.45 to 4.05 V/cm, through both energy-transfer resonances at 3.0 and 3.4 V/cm. The process is monitored by detecting one of the final products of resonant energy transfer, $34p_{3/2}$ atoms, with a selective field-ionization pulse applied 3 μs after the second dye laser pulse.

The objective of this experiment is to determine if the interaction of Eq. (4), which we can control, has an effect on the linewidth of the observed energy-transfer resonances. A prerequisite is that the strength of the interaction of Eq. (4)

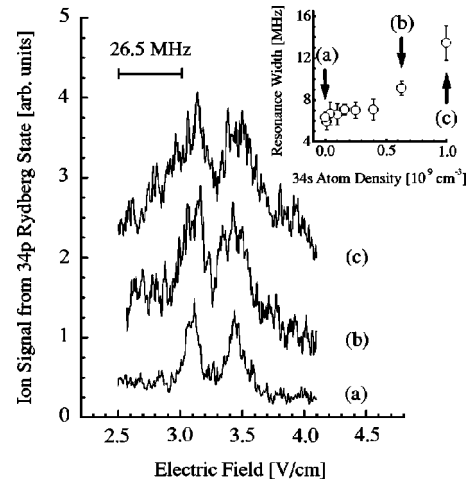


FIG. 2. Energy-transfer resonances of Eq. (1) for different densities of $\text{Rb}(34s)$ atoms. (a) Signal without microwave pulse. Estimated densities of $\text{Rb}(34s)$ atoms: (b) 6.3×10^8 cm⁻³, (c) 10^9 cm⁻³. The traces are shifted vertically. The inset shows the width of the observed resonances vs the estimated density of $\text{Rb}(34s)$ atoms. The arrows indicate the density of $\text{Rb}(34s)$ atoms, which generate the three resonances.

can be made larger than those of Eqs. (2) and (3). When $n[\text{Rb}(25s)]$ is comparable to $n[\text{Rb}(33s)]$, the interaction in Eq. (2) is 16 times stronger than the one in Eq. (3), and it was thought to be the main contribution to the broadening in the previous experiment [1]. To minimize this many-body interaction, the $25s$ state is excited with much lower density by attenuating the second dye laser intensity to fulfill the following condition, $n[\text{Rb}(25s)]\mu^2 \leq n[\text{Rb}(33s)]\mu'^2$, throughout the experiments discussed in this paper. Under these conditions we can expect to see the effect of the interaction of Eq. (4).

We excite the $33s$ state with the maximum dye laser power, which gives a density of about 5×10^9 $33s$ atoms/cm³, while the density of the $25s$ state is 40 times smaller, about 1.25×10^8 atoms/cm³, giving the most probable interatomic spacing $\bar{R}_{33s,33s} = ((4\pi/3)n[\text{Rb}(33s)])^{-1/3}$ and $\bar{R}_{25s,25s} = ((4\pi/3)n[\text{Rb}(25s)])^{-1/3}$. Under these conditions, any broadening effects from $25s$ atoms are negligible. Due to the huge difference between the densities of the $25s$ state and the $33s$ state, it is the number of $25s$ atoms that control how many resonant energy transfers occur. The most probable distance from a $25s$ atom to a $33s$ atom is determined by the $33s$ density, and $\bar{R}_{25s,33s} \approx \bar{R}_{33s,33s}$. Then, we have the most probable interaction strengths $\bar{V}_1 = \mu\mu'/\bar{R}_{25s,33s}^3 = 1.27$ MHz, $\bar{V}_2 = \mu^2/\bar{R}_{25s,25s}^3 = 0.12$ MHz, and $\bar{V}_3 = \mu'^2/\bar{R}_{33s,33s}^3 = 0.32$ MHz. When we excite $34s$ atoms the most probable distance of a $34s$ atom from a $33s$ - $25s$ pair is $\bar{R}_{34s,25s} = ((4\pi/3)n[\text{Rb}(34s)])^{-1/3}$, and the corresponding average interaction strength of Eq. (4) is $\bar{V}_4 = \mu'^2/\bar{R}_{34s,25s}^3$, which attains its maximum value of 3.53 MHz at the highest $34s$ density, 10^9 atoms/cm³.

Figure 2 shows the energy-transfer resonances taken with three different $34s$ densities. The conversion from field to

frequency at $E=3.4$ V/cm is 1 V/cm=53 MHz. It is evident that the width of the resonances increases with $34s$ density. The inset of Fig. 2 shows the increase of the resonance linewidth from 6 to 13.5 MHz as the density of $34s$ atoms is varied from 0 to 10^9 atoms/cm³. The densities for the three resonances shown are indicated by arrows in the inset. At $34s$ densities less than 0.35×10^9 cm⁻³, the broadening effect from $34s$ atoms is less than that from other sources. The instrumental width of the resonances, at very low $25s$ and $33s$ densities is 5 MHz, and we attribute it primarily to the magnetic-field inhomogeneity [9]. For the maximum $33s$ density and very low $25s$ density, the interaction \bar{V}_1 also contributes to the width, and for the data of Fig. 2, $2\bar{V}_1=2.5$ MHz. As the density of the $34s$ state increases to a critical value of 0.35×10^9 cm⁻³, where $n[\text{Rb}(34s)]\mu''^2 \approx n[\text{Rb}(33s)]\mu\mu'$ or $\bar{V}_4=\bar{V}_1$, the linewidth of the resonances starts to increase with increasing $34s$ density. This increase of the linewidth directly demonstrates the many-body nature of the resonant energy transfer. Note that, unlike pressure broadening, a higher $34s$ density not only increases the width of the resonances, but their amplitudes as well, as shown by Fig. 2.

We now address the question of why the always resonant interactions of Eqs. (2)–(4) increase the linewidths and amplitudes of the energy-transfer resonances of Eq. (1). The simplest model which contains the essential physics is one based on three atoms. Specifically, we choose the three-atom configuration shown in Fig. 3(a), in which the three atoms A , B , and C , are in the $25s$, $33s$, and $33s$, states, respectively. With this choice of states, only the interactions of Eqs. (1) and (3) play a role. We further assume that the A - C separation, R_{AC} , is at least twice the A - B separation R_{AB} . The difference between the R_{AB} and R_{AC} distances reflects the fact that the random spacing of our atoms leads to a distribution of interatomic spacings. The initial state is written in order as $\Psi_i = \Psi_{25s}^A \Psi_{33s}^B \Psi_{33s}^C$, and the two possible final states are $\Psi_f = \Psi_{24p}^A \Psi_{34p}^B \Psi_{33s}^C$ and $\Psi_{f'} = \Psi_{24p}^A \Psi_{33s}^B \Psi_{34p}^C$. The two states Ψ_f and $\Psi_{f'}$ both contain a $34p$ atom and both exhibit large Stark shifts, as implied by Fig. 1(a). It is useful to plot the energies of the eigenstates of this system versus the field in the vicinity of the resonance at 3.0 V/cm. First consider the case in which we ignore the couplings of Eqs. (1) and (3). The two final states are everywhere degenerate, and they cross the initial state at the resonance field, as shown by Fig. 3(b). Of course, with no coupling there is not an observable energy-transfer resonance.

Now we consider the case in which the couplings of Eqs. (1) and (3) are present, and $V_1 > V_3$, the usual situation when only $25s$ and $33s$ atoms are present initially. The energy levels are shown in Fig. 3(c). The coupling of Eq. (3) lifts the degeneracy of the final states, and away from the resonance, they are split by $2V_3 = 2\mu'^2/R_{BC}^3$. At the resonance, the coupling of Eq. (1) strongly couples atoms A and B with coupling $V_1 = \mu\mu'/R_{AB}^3 \gg V_3$; $\Psi_{f'}$ is therefore effectively decoupled from the other two states and can be ignored. There is in effect only one avoided crossing, between Ψ_i and Ψ_f . The eigenstates of this avoided crossing are approximately $\Psi_{1,2} = (\Psi_i \pm \Psi_f)/\sqrt{2}$ and $\Psi_{f'}$. The state initially excited by the laser is Ψ_i , which is the coherent superposition of Ψ_1 and

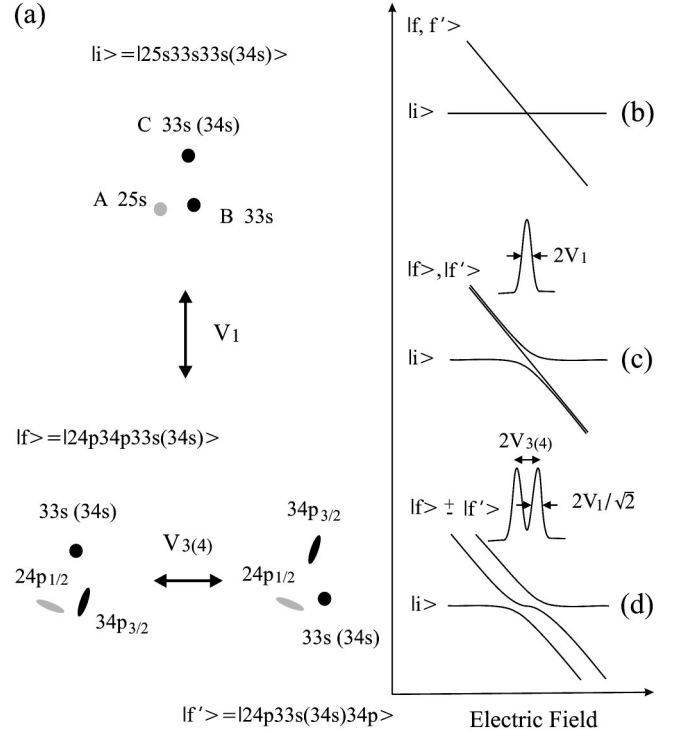


FIG. 3. (a) Physical locations of three atoms in the $25s$, $33s$, and $33s$ (or $34s$) states, comprising the initial state $|i\rangle$. The coupling V_1 connects the atoms into the two possible final states $|f\rangle$ and $|f'\rangle$, which are coupled by the interaction V_3 (or V_4). (b–d) Energy levels vs tuning field E : (b) all coupling vanish so that $|f\rangle$ and $|f'\rangle$ are degenerate and cross $|i\rangle$ so that no energy transfer occurs; (c) $V_1 > V_3$ (atom C in $33s$ state), off resonance $|f\rangle$ and $|f'\rangle$ are weakly coupled but on resonance, $|i\rangle$ and $|f\rangle$ are strongly coupled, and $|f'\rangle$ is decoupled from the other two states, leading to an energy-transfer resonance of width $2V_1$ and amplitude $1/2$; and (d) $V_4 > V_1$ (atom C now in $34s$ state), the $|f\rangle$ - $|f'\rangle$ coupling is strong enough that there are two resolved resonances, each of width $2V_1/\sqrt{2}$, and amplitude $1/2$.

Ψ_2 , and the state of the system oscillates between Ψ_i and Ψ_f at the frequency $2V_1$. In the real experiment, there are many pairs of atoms and a range of values of V_1 , so it is impossible to observe the oscillation between Ψ_i and Ψ_f . To mimic this situation with the three atoms of Fig. 3, we can calculate the time-average probability of finding the system in Ψ_f for times long compared to $1/2V_1$. In this case, as we tune through the resonance we see essentially one transition, between Ψ_i and Ψ_f , with width $2V_1 = 2\mu\mu'/R_{AB}^3$ and amplitude $1/2$.

If $V_1 \gg V_3$, the effect of atom C at the resonance can be ignored, but if atom C is a $34s$ atom instead of a $33s$ atom, as shown in Fig. 3(a), it plays a crucial role. The initial state is now $\Psi_i = \Psi_{25s}^A \Psi_{33s}^B \Psi_{34s}^C$, while the two possible final states are $\Psi_f = \Psi_{24p}^A \Psi_{34p}^B \Psi_{33s}^C$, $\Psi_{f'} = \Psi_{24p}^A \Psi_{33s}^B \Psi_{34p}^C$, which are coupled to each other through Eq. (4) with the interaction strength $V_4 = \mu''^2/R_{BC}^3$. Due to the large value of μ'' , it is straightforward to vary V_4 from $V_4 \ll V_1$ to $V_4 \gg V_1$ by changing the density of $34s$ atoms. When $V_4 < V_1$ the energy levels are similar to those shown in Fig. 3(c), and one resonance of width $2V_1$, is observed. However, when $V_4 > V_1$ the energy

levels are very different, as shown in Fig. 3(d). Away from the resonance, the final eigenstates are linear superpositions $(\Psi_f \pm \Psi_{f'})/\sqrt{2}$, which are separated in energy by $2V_4$. As the initial state is scanned past these final states, there is not one, but two avoided crossings, separated by $2\mu'^2/R_{BC}^3=2V_4$, and two resonances are observed. The width of each resonance is given by $2V_1/\sqrt{2}=2\mu\mu'/R_{AB}^3/\sqrt{2}$, but the amplitude is still $1/2$. Since there are now two resonances, the total area of the signal is increased by a factor $2 \times (1/\sqrt{2})=\sqrt{2}$. In our experiments, there are not three, but many atoms, and the spacings analogous to R_{BC} are random. Consequently, there are not two, but many possible final states, and they expand into an energy band of width Δ , since there are simultaneous interactions involving atoms with a broad range of separations [10]. The linewidth of the transition is given by the width of the energy band Δ , which is substantially broader than the two-body interaction V_1 .

To verify that the three-atom model of Fig. 3 captures the essential physics, we have carried out a computer simulation of our experiment. In the first case, initially atom *A* is a 25*s* atom, and atoms *B* and *C* are 33*s* atoms. R_{AB} is about the average separation in our experiment, leading to the interaction strength $V_1=1.28$ MHz, and $R_{BC} \approx R_{AC} \sim 1.8 R_{AB}$. Under these conditions, atom *C* is effectively decoupled from atoms *A* and *B*, whether they are in the 25*s* and 33*s* states or the 24*p* and 34*p* states. In the second case, atom *C* is a 34*s* atom instead of a 33*s* atom. In this case, atom *C* is strongly coupled to atom *B* when it is in the 34*p* state (i.e., the $\Psi_{f \pm} \Psi_{f'}$ coupling described earlier). In both cases, we calculate the average long-time transition probability from the initial state to states in which two of the atoms are in the final 24*p* and 34*p* states. In the first case, which corresponds to the schematic resonance shown in Fig. 3(c), where there is no 34*s* state population, the resonance is shown by the dotted line of Fig. 4. In the second case, for a specific R_{BC} spacing, we see the double peaks predicted in Fig. 3(d), as shown by the dashed-dotted line of Fig. 4. To simulate the conditions of the experiment, in which there are many 34*s* atoms randomly distributed, we have averaged the result of the calculations for spacings ranging from half of the average spacing to two times the average spacing of 34*s* to a 33*s*-25*s* pair,

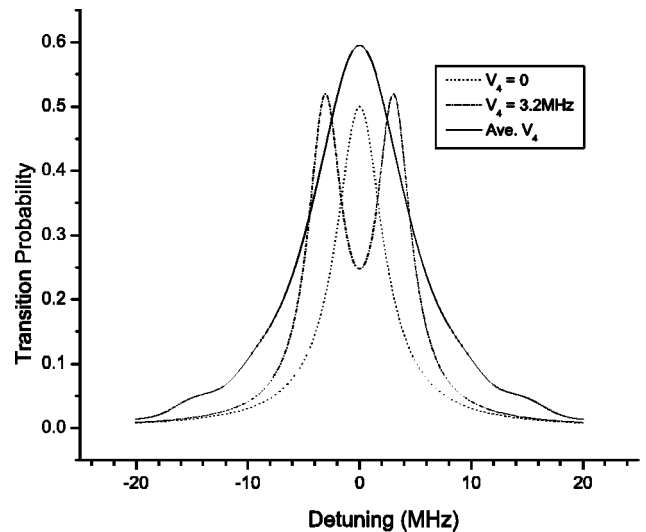


FIG. 4. The simulated long-time average resonant energy-transfer probability. The dotted line, the resonance without 34*s* atoms, is about 5-MHz wide; the dashed-dotted line, the resonance with $V_4=3.2$ MHz, has double peaks; the solid line, the resonance averaged over a range of V_4 strength, is about 10-MHz wide, and increased in amplitude.

yielding the solid line of Fig. 4. The simulated resonance shown in Fig. 4 is in good qualitative agreement with our observations of Figs. 2(b) and 2(c), i.e., adding 34*s* atoms not only broadens the resonance but increases its area as well.

In conclusion, introducing an additional 34*s* state into the resonant energy-transfer process provides decisive evidence that the dipole-dipole couplings in a frozen Rydberg gas have the nature of a many-body interaction. Further systematic study of interactions in this cold Rydberg sample, particularly using microwaves, is under way.

It is a pleasure to acknowledge helpful discussions with V. Celli, R.R. Jones, P. Pillet, P. Tanner, and R.W. Field during the course of this work. We thank M.W. Noel for participation in building the MOT. This work has been supported by the U. S. Air Force Office of Scientific Research.

- [1] W. R. Anderson, J. R. Veale, and T. F. Gallagher, Phys. Rev. Lett. **80**, 249 (1998).
- [2] I. Mourachko, D. Comparat, F. de Tomasi, A. Fioretti, P. Nosbaum, V. M. Akulin, and P. Pillet, Phys. Rev. Lett. **80**, 253 (1998).
- [3] M. P. Robinson, B. Laburthe Tolra, M. W. Noel, T. F. Gallagher, and P. Pillet, Phys. Rev. Lett. **85**, 4466 (2000).
- [4] T. C. Killian, M. J. Lim, S. Kulin, R. Dumkes, S. D. Bergeson, and S. L. Rolston, Phys. Rev. Lett. **86**, 3759 (2001).
- [5] T. F. Gallagher, Phys. Rep. **210**, 319 (1992).

- [6] R. H. Dicke, Phys. Rev. **93**, 99 (1954).
- [7] D. Jaksch, J. J. Cirac, P. Zoller, S. L. Rolston, R. Côté, and M. D. Lukin, Phys. Rev. Lett. **85**, 2208 (2000).
- [8] M. D. Lukin, M. Fleishauser, R. Côté, L. M. Duan, D. Jaksch, J. J. Cirac, and P. Zoller, Phys. Rev. Lett. **87**, 037901 (2001).
- [9] W. Li, I. Mourachko, M. W. Noel, and T. F. Gallagher, Phys. Rev. A **67**, 052502 (2003).
- [10] V. M. Akulin, F. de Tomasi, I. Mourachko, and P. Pillet, Physica D **131**, 125 (1999).